Radiation Physics and Chemistry 155 (2019) 146–149

Contents lists available at ScienceDirect

Radiation Physics and Chemistry

journal homepage: www.elsevier.com/locate/radphyschem

# Fabrication and characterization of Schott Borofloat® 33 microstrip electrodes

Nathaniel S. Edwards[a,*], Benjamin W. Montag[a,b], Luke C. Henson[b], Steven L. Bellinger[a,b], Daniel M. Nichols[a], Michael A. Reichenberger[a], Ryan G. Fronk[a], Douglas S. McGregor[a]

[a] Semiconductor Materials and Radiological Technologies (S.M.A.R.T.) Laboratory, Kansas State University, Department of Mechanical and Nuclear Engineering, 3002 Rathbone Hall, 1701B Platt Street, Manhattan, KS 66506, USA
[b] Radiation Detection Technologies, Inc., 4615 S. Dwight Dr., Manhattan, KS 66502, USA

ARTICLE INFO

*Keywords:*
Microstrip electrodes
Electrode fabrication
Electrode characterization
Electrical stability

ABSTRACT

Microstrip electrodes fabricated using Schott Borofloat® 33 as the electrode substrate were recently characterized in order to optimize the performance of $^{6}$Li-based suspended foil microstrip neutron detectors. The Schott Borofloat® 33 microstrip electrode capacitance was measured to be 67 pF before characterization efforts were conducted using a collimated $^{241}$Am alpha-particle source positioned between the microstrip electrode and a planar drift electrode. Characterization studies were performed to define counting and gas multiplication curves as well as study the electrical stability of the microstrip electrode substrate. Electrical stability was observed for approximately 23 h after the initial hour testing. A non-uniform drift electric field strength distribution was observed by measuring the pulse amplitude from a collimated $^{241}$Am alpha-particle source positioned at five discrete positions along the span of the drift electric field region between the microstrip and drift electrodes. All measurements were conducted within a sealed aluminum enclosure backfilled with P-10 gas.

## 1. Introduction

Microstrip electrodes were first introduced by Oed in 1988 (Oed, 1988) as an alternative electrode design to multi-wire proportional counters (MWPCs). The microstrip electrode design operates on the principle of a high electric field region, of sufficient strength to cause Townsend avalanching, being formed by the potential difference between neighboring metal anode and cathode strips positioned less than 1 mm apart from one another (Oed, 1988). An illustration of a microstrip electrode is shown in Fig. 1 and depicts the interdigitated orientation of neighboring anode and cathode strips. The advantage of the microstrip electrodes over MWPCs is the distance between neighboring anode and cathode strips can be reduced below the limiting distance between neighboring wires in MWPCs (Oed, 1988), and, therefore, allows for improved spatial resolution.

Previously, $^{6}$Li-based suspended foil microstrip neutron detectors (SFMNDs) were fabricated and tested using a microstrip electrode fabricated atop a silicon substrate with a 3-μm thick $SiO_2$ layers on both surfaces of the substrate (Edwards et al., 2016). Ionic charging of the microstrip electrode was observed as indicated by the gradual reduction in signal amplitude as a function of time (Edwards et al., 2016; Oed et al., 1989; Oed, 1995). Additionally, the microstrip electrode had a measured capacitance of approximately 750 pF which may have resulted in a poor signal-to-noise ratio causing lower-energy events to blend with electronic noise (Edwards et al., 2016). Therefore, this report focuses on the selection of an electrically stable microstrip-electrode substrate and the subsequent fabrication and characterization of the microstrip electrodes using the same photolithography pattern and strip metals previously used for the silicon-based microstrip electrodes (Edwards et al., 2016).

## 2. Microstrip-electrode fabrication

Proper selection of an electrically stable microstrip-electrode substrate was crucial prior to fabricating the microstrip electrodes. Other works have relied on glass substrates such as Schott S8900 and Corning 7740 which possess electrical stability for at least several hours (Oed, 1995; Gong et al., 1994). However, despite its electrical capability (Oed, 1995; Gong et al., 1994; Ortuño-Prados and Budtz-Jørgensen, 1995), Schott S8900 is not a common type of glass and, as a result, is rather expensive compared to other common microstrip-electrode substrate materials such as silicon and Corning 7740. Corning 7740 is another well-known electrically stable microstrip-electrode substrate; however production of the substrate material has ceased and thus the

* Corresponding author.
*E-mail address:* nedwards@ksu.edu (N.S. Edwards).

https://doi.org/10.1016/j.radphyschem.2018.10.016
Received 31 July 2017; Received in revised form 19 October 2018; Accepted 19 October 2018
Available online 23 October 2018
0969-806X/ 

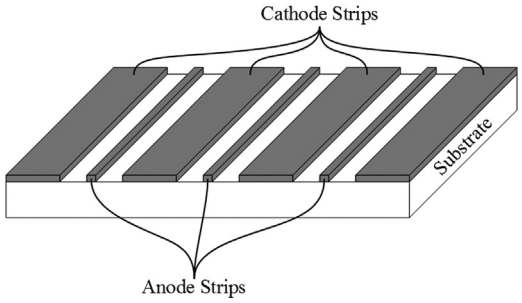


**Fig. 1.** Microstrip electrode containing interdigitated anode and cathode strips fabricated via standard metal lift-off photolithography processes.

**Table 1**
Comparison of the composition of Borofloat® 33 (Schott, 2017) and Corning 7740 (Corning, 2009) glasses.

| Name | Chemical composition (%) | |
|---|---|---|
| Schott Borofloat® 33 | $SiO_2$ | (81) |
| | $B_2O_3$ | (13) |
| | $Na_2O/K_2O$ | (4) |
| | $Al_2O_3$ | (2) |
| Corning 7740 | $SiO_2$ | (80.6) |
| | $B_2O_3$ | (13.0) |
| | $Na_2O$ | (4.0) |
| | $Al_2O_3$ | (2.3) |
| | Misc. Traces | (0.1) |

material is no longer available. Recently, Schott began producing a glass substrate named Borofloat® 33 (Schott, 2017) that has nearly identical composition to Corning 7740 (Corning, 2009), as listed in Table 1.

The 4.2 cm × 4.2 cm microstrip electrodes were fabricated in the Kansas State University Semiconductor Materials And Radiological Technologies (S.M.A.R.T.) Laboratory class 100 clean room on a 100-mm diameter, 500-μm thick Schott Borofloat® 33 substrate using standard metal-liftoff photolithography processes (Ghandhi, 1994), as illustrated in Fig. 2. As shown in Fig. 3, the microstrip electrodes contained 25-μm wide anode strips and 500-μm wide cathode strips with an anode-to-anode pitch of 1000 μm. Additionally, the microstrip anode and cathode strips and drift electrode were deposited using electron-beam evaporation and the metals used were Cr, Cu, and Au at thicknesses of 500 Å, 3000 Å, and 1000 Å, respectively. As shown in the center of Fig. 3, all of the anode strips were interconnected and read out through a single 2 mm × 2 mm bond pad located in the bottom left of the image. Similarly, all of the cathode strips were interconnected to a single 2 mm × 2 mm bond pad located in the top right of the image. The spacing between anode (A) and cathode (C) strips was maintained throughout the length of the strips as well as at the ends of the strips as shown on the right of Fig. 3.

## 3. Microstrip electrode characterization

Prior to conducting electrode-characterization studies, the capacitance of the Schott Borofloat® 33 microstrip electrodes was measured using an Agilent U1731C LCR meter. The measured electrode capacitance was 67 pF for a test voltage of approximately 0.7 $V_{rms}$ (Agilent, 2012).

### 3.1. Counting and gas multiplication curves

Counting and gas multiplication curves were simultaneously defined using the test configuration depicted in Fig. 4. The Schott Borofloat® 33 microstrip electrode was positioned at a distance of 4 cm from a planar drift electrode using a plastic support structure to maintain the

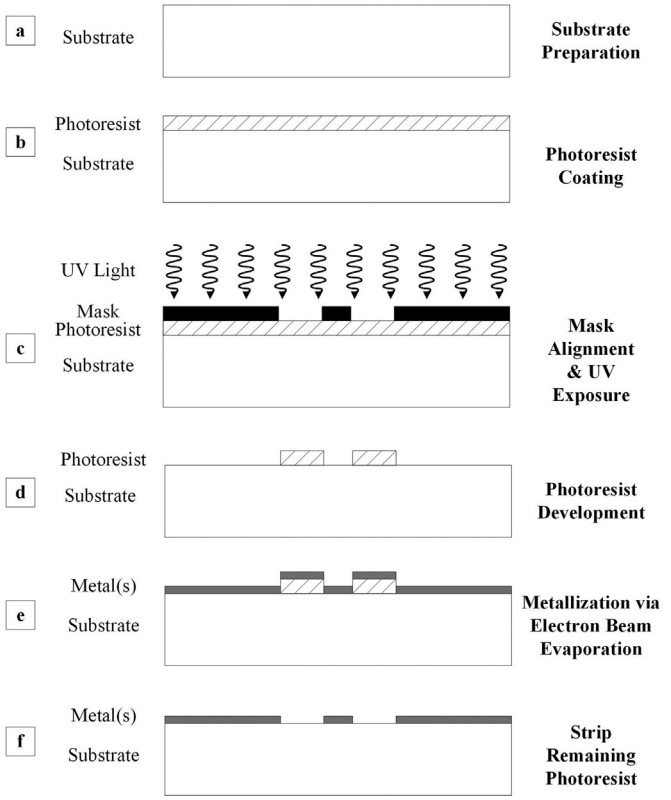


**Fig. 2.** Microstrip electrode fabrication steps using standard metal lift-off photolithography processes.

positions of the microstrip and drift electrodes. A collimated $^{241}Am$ alpha-particle source was positioned 19 mm above the microstrip electrode surface at a distance of 20 mm from the edge of the vertically aligned microstrip and drift electrodes (and therefore the edge of the drift electric field) to inject approximately 3.6 MeV of energy within the drift electric field region, based on the characteristic Bragg curve of alpha particles (Ziegler and Biersack, 2013). The aperture of the collimator was approximately 2.5 mm. The test setup was contained within a sealed aluminum enclosure pressurized with 3.7 psig (1.25 atm) of P-10 proportional gas (90% argon, 10% methane). Both curves, shown in Fig. 5, were defined by increasing the anode strip applied voltage from 0 to 540 V in 20-volt increments. The cathode strips were maintained at ground potential and the drift electrode was maintained at −1000 V throughout the duration of the measurements. The gas multiplication curve was defined by calculating the ratio of the measured pulse amplitude for a given applied voltage setting, $V_i$, to the initial pulse amplitude, $V_O$, at an applied voltage of approximately 0 V (ratio defined as $V_i/V_O$).

### 3.2. Electrical stability measurements

The testing configuration illustrated in Fig. 4 was also used to compare the electrical stability of the Schott Borofloat® 33 and silicon-based microstrip electrodes (Edwards et al., 2016) by monitoring the measured pulse amplitude from a collimated $^{241}Am$ alpha-particle source for approximately 24 h. Each electrode was separately tested within a sealed aluminum enclosure pressurized with 3.7 psig (1.25 atm) of P-10 proportional gas and again the cathode strips were maintained at ground potential with the drift electrode maintained at −1000 V throughout the duration of the testing. The Schott Borofloat® 33 anode strips were maintained at 400 V while the silicon-based microstrip anode strips were maintained at 300 V throughout the duration of the testing.

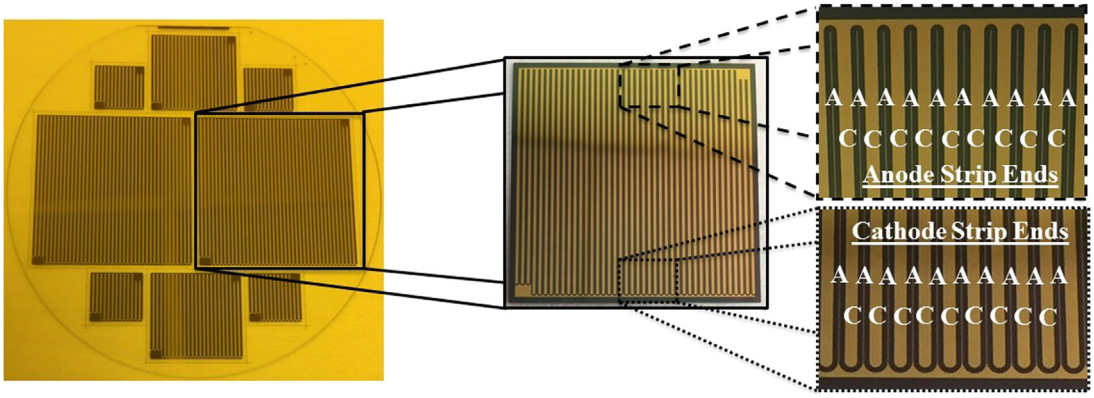


**Fig. 3.** Microstrip electrodes fabricated on a 100-mm diameter, 500-μm thick Schott Borofloat® 33 substrate.

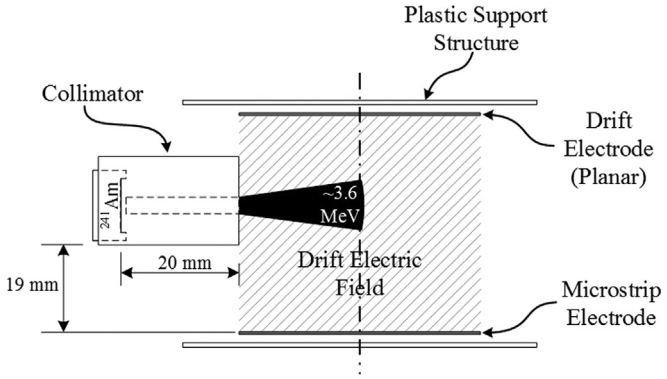


**Fig. 4.** Illustration of the experimental configuration required to define the counting and gas multiplication curves using the Schott Borofloat® 33 microstrip electrode positioned at a distance of 4 cm from the planar drift electrode.

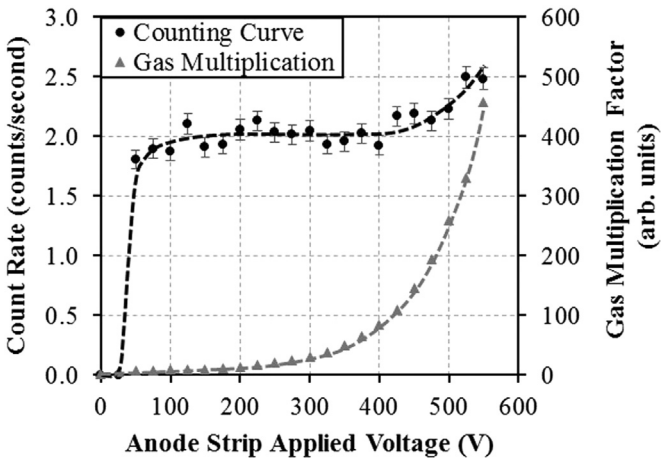


**Fig. 5.** Measured counting and gas multiplication curves using the Schott Borofloat® 33 microstrip electrode for various anode strip applied voltages.

Shown in Fig. 6 is the relative gain of the Schott Borofloat® 33 microstrip electrode as a function of time compared to the silicon-based microstrip electrode. Both microstrip electrodes exhibited an initial duration of time of approximately 1 h for the electrodes to reach a stable operating condition. The Schott Borofloat® 33 microstrip electrode remained electrically stable for a duration of time of approximately 23 h following the initial hour. However, the relative gain of the silicon-based microstrip electrode began to decrease immediately after the first hour of operation (when the relative gain initially increases) due to ionic charging of the $SiO_2$ surface layer (Oed et al., 1989; Oed, 1995).

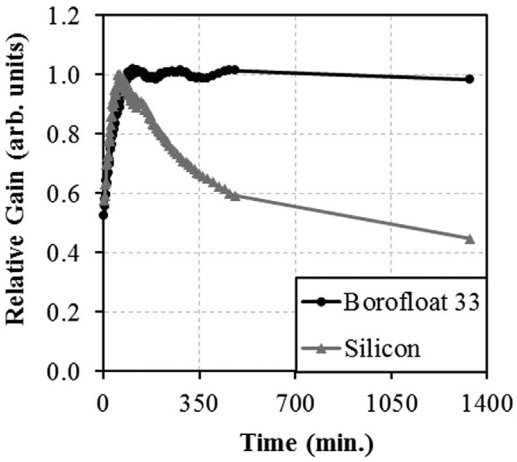


**Fig. 6.** Normalized microstrip electrode gain as a function of time. The electrical stability of a silicon-based microstrip electrode and a Schott Borofloat® 33-based microstrip electrode were each measured separately. In each measurement scenario, the operating voltage (anode and cathode strips, and drift electrode applied voltage settings) was maintained for approximately 24 h.

### 3.3. Drift electric field probing

The distribution of the drift electric field strength between an anode (either planar electrode or Schott Borofloat® microstrip electrode) and the planar, drift electrode was measured using the experimental setup depicted in Fig. 7. The anode and drift electrode were positioned 4 cm apart from one another and contained within a sealed aluminum enclosure pressurized with 1.0 psig (1.07 atm) of P-10 proportional gas. A

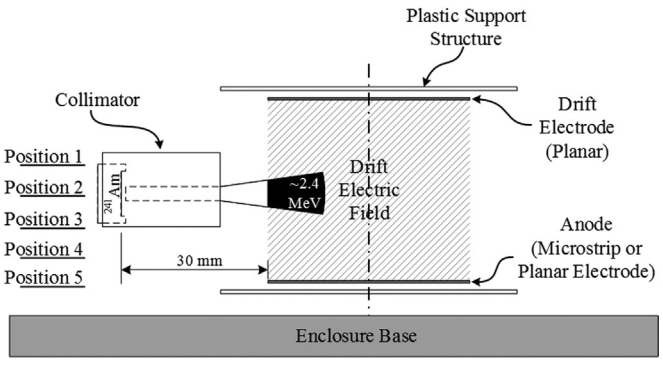


**Fig. 7.** Illustration of the experimental configuration used for measuring the drift electric field strength distribution between an anode (either planar electrode or Schott Borofloat® 33 microstrip electrode) and the planar, drift electrode.

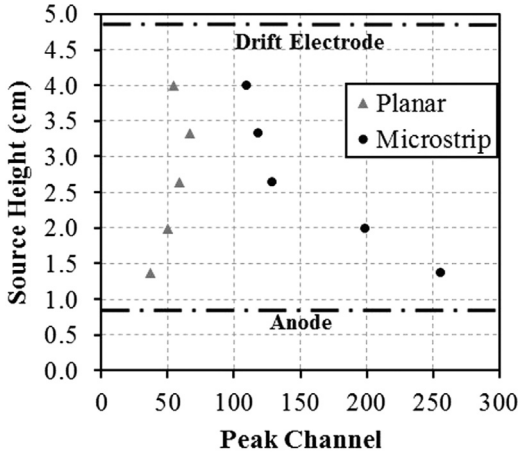


**Fig. 8.** Comparison of the distribution of measured pulse amplitude (peak channel) as a function of the position of a collimated $^{241}$Am alpha-particle source for an anode using a planar electrode and a Schott Borofloat® 33 microstrip electrode.

collimated $^{241}$Am alpha-particle source was positioned at a distance of 30 mm from the edge of the vertically aligned anode and drift electrode to inject approximately 2.4 MeV of energy within the drift electric field region, based on the characteristic Bragg curve of alpha particles (Ziegler and Biersack, 2013). The collimated $^{241}$Am alpha particle source was positioned at five discrete vertical positions along the length of the drift electric field region. The distance separating the source from the edge of the vertically-aligned electrodes was increased, relative to the distance used for the data shown in Figs. 5 and 6, to accommodate the source collimator at the highest and lowest source positions. The drift electrode was maintained at −1000 V and the anode (either planar electrode or Schott Borofloat® 33 microstrip electrode anode strips) was operated at 400 V for all measurements. The cathode strips were maintained at ground potential when using the Schott Borofloat® 33 microstrip electrode. The configuration and settings of the NIM equipment that were used to conduct the measurements were identical for both anode types. Measurements were performed after an initial one-hour duration of time for the electrode setup to reach a stable operating condition.

Fig. 8 shows the distribution of measured pulse amplitudes, indicated on the *x*-axis as "Peak Channel" of Fig. 8. The peak channel of each source position corresponds to the most prominent channel of the measured pulse-height spectrum using Ortec's multi-channel analyzer program Maestro®. The Schott Borofloat® 33 microstrip electrode scenario shows a slight increase in pulse amplitude until approximately half-way between the drift and microstrip electrodes (source height of approximately 2.6 cm) before the pulse amplitudes increase more significantly as the collimated $^{241}$Am alpha-particle source is positioned closer to the microstrip electrode surface. Given that high-outgassing, polymer-based materials were used to construct the test fixture, there is concern that electron attachment may have occurred (Rice-Evans, 1974; Christophorou, 1971) resulting in a degradation in pulse amplitude as the collimated $^{241}$Am alpha-particle source is positioned further away from the microstrip electrode surface. However, the distribution of measured pulse amplitudes as a function of source height for the planar scenario still behaved consistent with a parallel-plate ionization chamber (Tsoulfanidis, 1995; Knoll, 2010).

## 4. Conclusions

Schott Borofloat® 33 has been identified and used as a substrate for the fabrication of microstrip electrodes that exhibits electrical stability for a minimum duration of time of approximately 23 h. Additionally, the use of Schott Borofloat® 33 as a microstrip electrode substrate has resulted in the reduction in microstrip electrode capacitance from approximately 750 pF for a silicon-based microstrip electrode to 67 pF for a Schott Borofloat® 33 microstrip electrode with identical strip geometry and metals. The Schott Borofloat® 33 microstrip electrode, when positioned at a distance of 4 cm from a planar drift electrode, exhibited a non-uniform pulse-height distribution which was measured using a collimated $^{241}$Am alpha particle source.

It is currently uncertain as to the cause of the non-uniform distribution of pulse amplitudes measured from a collimated $^{241}$Am alpha-particle source positioned at five discrete positions along the drift electric field region. However, electron attachment is suspected to be occurring within the drift electric field region between the microstrip and drift electrodes. Future studies will involve the replacement of all polymer-based materials contained within the sealed test enclosure with low-outgassing materials in an attempt to determine the significance, if any, of electron attachment within the system. Although the capacitance of the microstrip electrode was reduced to 67 pF by using Schott Borofloat® 33 as the substrate, further improvements to reduce the microstrip electrode capacitance, and thus increase the signal-to-noise ratio, are desired.

## Acknowledgements

Fabrication and characterization of microstrip electrodes was conducted at the Kansas State University Semiconductor Materials and Radiological Technologies (S.M.A.R.T.) Laboratory.

## References

Agilent, 2012. Agilent U1731C, U1732C, and U1733C Handheld LCR Meter, Agilent Technologies. (Online). Available: 〈http://www.sophphx.caltech.edu/Lab_Equipment/Agilent_U1731C_LCR_Meter.pdf〉. (Accessed 9 October 2018).

Christophorou, L.G., 1971. Atomic and Molecular Radiation Physics. John Wiley & Sons, Inc, Canada.

Corning, 2009. Properties of PYREX®, PYREXPLUS® and Low Actinic PYREX Code 7740 Glasses, National Scientific Company. (Online). Available: 〈www.quartz.com/pxprop.pdf〉. (Accessed 24 July 2017).

Edwards, N.S., Montag, B.W., Henson, L.C., Bellinger, S.L., Fronk R.G., Reichenberger, M. A., McGregor, D.S., 2016. Lithium foil gas-filled neutron detector using microstrip electrodes. In: Proceedings of the Conference Rec. IEEE Nuclear Science Symposium, Strasbourg, France, Oct. 29 – Nov. 5, 2016.

Ghandhi, S.K., 1994. VLSI Fabrication Principles: Silicon and Gallium Arsenide. John Wiley & Sons, Inc, Canada.

Gong, W.G., Wieman, H., Harris, J.W., Mitchell, J.T., Hong, W.S., Perez-Mendez, V., 1994. Microstrip gas chambers on glass and ceramic substrates. IEEE Trans. Nucl. Sci. NS 41 (4), 890–897.

Knoll, G.F., 2010. Radiation Detection and Measurement, 4th ed. John Wiley & Sons, Inc, Hoboken, NJ.

Oed, A., Convert, P., Berneron, M., Junk, H., Budtz-Jørgensen, C., Madsen, M.M., Jonasson, P., Schnopper, H.W., 1989. A new position sensitive proportional counter with microstrip anode for neutron detection. Nucl. Instrum. Methods Phys. Res. A 284 (1), 223–226.

Oed, A., 1988. Position-sensitive detector with microstrip anode for electron multiplication with gases. Nucl. Instrum. Methods Phys. Res. A 263 (2), 351–359.

Oed, A., 1995. Properties of micro-strip gas chambers (MSGC) and recent developments. Nucl. Instrum. Methods Phys. Res. A 367 (1–3), 34–40.

Ortuño-Prados, F., Budtz-Jørgensen, C., 1995. The electron-conducting glass SCHOTT S8900 as substrata for microstrop gas chamber. Nucl. Instrum. Methods Phys. Res. A 364 (2), 287–289.

Rice-Evans, P., 1974. Spark, Streamer, Proportional and Drift Chambers. The Richelieu Press Limited, London.

Schott, 2017. BOROFLOAT® 33 – General Information, Schott Technical Glass. (Online). Available: 〈https://www.schott.com/d/borofloat/b2c50cc4-74a1-4c31-8af3-c7de01877182/1.0/borofloat33_gen_eng_web.pdf〉. (Accessed 24 July 2017).

Tsoulfanidis, N., 1995. Measurement and Detection of Radiation, 2nd ed. Taylor & Francis, Washington, D.C.

Ziegler, J.F., Biersack, J.P., 2013. SRIM-2013 Code. IBM Company.